Nonlinear state observer for estimating and controlling of friction-induced vibrations

Lyes Nechak

Nonlinear state observer for estimating and controlling of friction-induced vibrations

Lyes Nechak[a]

[a]*Laboratoire de Tribologie et Dynamique des Systèmes, UMR CNRS 5513, École Centrale de Lyon, 36 avenue Guy de Collongue 69134 Écully Cedex, France (e-mail: lyes.nechak@ec-lyon.fr).*

Abstract

This paper focuses on the nonlinear estimating of friction-induced vibrations (FIV) related to the mode-coupling mechanism. This task is a key step for implementing control laws when FIV are required to be mitigated. Then, this study proposes nonlinear state observers based on the gradient descent method. Two types are investigated: the first one is the gradient descent nonlinear observer (GDNLO) which gives estimations of vibrations by minimizing the gradient of the error between the system and observer outputs, while the second, called the modified GDNLO, gives estimations by minimizing the gradient of the errors between the high order derivatives of the system and observer outputs. Performances of both observers are analysed by considering the properties of their convergences when used for the estimation of the mode-coupling based vibrations and when used for controlling the vibrations via linearizing and stabilizing feedbacks. Based on numerical simulations, the modified GDNLO has shown better and more suitable convergence properties than the GDNLO. High accuracy levels are obtained for the estimated vibrations. Moreover, this accuracy is kept when the modified GDNLO is inserted in a control loop for the mitigating of the FIV.

Keywords: Nonlinear dynamical systems, Friction-induced vibration, mode-coupling, nonlinear state observer, gradient descent method, nonlinear control, feedback linearization.

1. Introduction

Fiction-induced vibrations (FIV) are required to be controlled in numerous engineering applications due to their negative impact on systems performances, varying from

acoustic discomfort to a degradation of systems and operating safety. Brake squeal, clutch chatter and vibrations in controlled positioning systems are well-known examples in this area.

Nowadays, it is common to classify FIV with respect to their origin into two main families [1, 2, 3]. The first one explains the vibrations from tribological view point by the variation of the friction coefficient against the relative velocity between the structures in contact. The variation from a static to a dynamic value can be discontinuous or can evolve according to a smoother relation as given by the Stribeck model, exponential or polynomial models [4, 5, 6, 7]. The second family points out the importance of structural aspects in the process of generating vibrations. Indeed, it was shown that these vibrations may occur even with a constant friction coefficient and are rather related to the so-called mode coupling phenomenon [1, 2, 8, 9]. The latter is characterized by the approximation in frequency of two modes until equality at a particular value of the friction coefficient called coalescence point. At this stage, a small perturbation of the equilibrium will drive the system to a stationary vibratory state.

Numerous studies have been devoted to the analysis and prediction of FIV in deterministic framework by using the complex eigenvalue analysis [10, 11, 12] or by using nonlinear transient analysis [13, 14]. The prediction of FIV in uncertain frameworks has also concentrated much of interest by using sensitivity approaches and probabilistic meta-models [15, 16, 17, 18], non-probabilistic meta-models [19, 20] or hybrid metamodels [21, 22] and fuzzy approaches [23]. The key aim of all these studies is to predict FIV in order to determine wether they can be neglected or must be mitigated or even suppressed.

Numerous schemes and methods have been proposed for efficient controlling of FIV. A passive control strategy was proposed in [24] for the mitigating of friction-induced stick-slip vibrations by means of the modulation of an externally imposed normal force. A similar approach proposed in [6] consisted in the using of a high frequency tangential external excitation. The using of a dynamic vibration absorber of stick-slip vibrations was proposed in [25] while Nonlinear Energy Sink (NES) was proposed in [26] for a passive mitigating of mode-coupling instabilities. Otherwise, structural modifications was also proposed in [27] and were shown to be not always well suitable for assigning the

system's eigenvalues to the desired locations, which makes the friction system difficult to be stabilized. Active control strategies offer different other schemes that can prove to be effective. The PID regulator proposed in [28] has shown unsatisfactory performances when used for suppressing stick-slip vibrations issued from the discontinuous evolution of friction coefficient from the static to the dynamic value, while the PID with a high gain has shown better aptitudes for suppressing stick-slip vibrations when the friction coefficient is smoothly depending on the relative sliding velocity [29]. Numerous other techniques based on linear delayed and non-delayed state feedbacks [30, 31, 32, 33, 34] were proposed for controlling FIV. Most of them define control loops which permit the assigning of the locations of the system eigenvalues to desired positions, imposing desired dynamical behaviours. A robust assigning of eigenvalues was proposed in [35]. Otherwise and more recently, linearizing state feedback based strategies were developed in [36] for the mitigating of mode-coupling instabilities. The main idea is to define a nonlinear coordinate transformation for simplifying the non-linearities and thus for putting the system into a linear form, the control of which can be performed more easily by using classical linear techniques. However, an effective implementation of this nonlinear scheme and even all linear and nonlinear state feedbacks for controlling FIV requires the latter to be measurable. For this purpose, using sensors is in numerous practical cases unsuitable due to either the infeasibility and/or the cost of the measures or to the high impact of sensors on the dynamical behaviour of the controlled system. Hence, using state observers becomes mandatory.

In fact, a state observer is a dynamical system which gives from the inputs and outputs of the system to be controlled, estimations of the state variables. The aim is then to use these estimations instead of measures that would be impossible or too expensive to perform, for the controlling of FIV. This issue and more particularly the controlling of stick-slip vibrations by using state observer was considered in a number of studies as in [37, 38, 39, 40]. Otherwise, the literature does not refer to any study dealing with the controlling of mode coupling instabilities by using nonlinear state observers. Hence, this paper focuses on this issue and proposes to investigate nonlinear observation and control schemes when combined together for the mitigating of FIV issued from the mode coupling mechanism. The linearizing feedback approach was proposed recently in [36]

for the controlling of mode-coupling instabilities. Then, this study proposes the implementing of this nonlinear control scheme by using a nonlinear state observer. The latter enjoys a reach literature [41]. The main issue concerning the using of nonlinear state observers for control objectives is related to the separation principle which is not systematically verified when dealing with control of nonlinear dynamical systems. In fact, by opposite to linear systems, the calculation of the state feedback and the state observer independently each other does not guarantee the stability of the whole closed loop system [42, 43]. Two types of state observers are studied in this paper. The first one, named GDNLO (gradient descent nonlinear observer) gives estimations of FIV in the direction minimizing the gradient of the error between the outputs of the friction system and the corresponding state observer while the second, called the modified GDNLO, offers the estimations by minimizing the gradient of the error between high order derivatives of the system and observer outputs. So, the main contributions of this paper are mainly related to the developing and the assessing of the gradient descent nonlinear based observers within the framework of active control of friction-induced vibrations issued from the mode-coupling mechanism. The corresponding objective consists in the analysis of the performances of gradient descent based observers ([44]) when used for the estimation of mode-coupling based vibrations and when inserted in control loops based on the linearizing and stabilizing state feedbacks, recently proposed in [36] for the mitigating of the vibrations.

This paper is organized as follows. First, a brief description of the considered nonlinear dynamical systems and the problem we are concerned, are given in Section 2 . Then, the GDNLO and the modified GDNLO are presented and developed in Section 3. Efficiency of both state observers in the estimating of FIV issued from the mode coupling mechanism is analyzed in Section 4. Performances of both observers when used in closed loops for the controlling of the vibrations are also discussed. Conclusion is given at the end of the paper.

2. Nonlinear dynamical systems and mathematical background

Consider mechanical systems described by the following second order differential equations:

$$\boldsymbol{M}\ddot{\boldsymbol{X}} + \boldsymbol{C}\dot{\boldsymbol{X}} + \boldsymbol{K}\boldsymbol{X} + \boldsymbol{F}_{\mathrm{NL}}(\boldsymbol{X}) = \boldsymbol{B}u \tag{1}$$

where $\boldsymbol{M}$, $\boldsymbol{C}$ and $\boldsymbol{K}$ are the mass, damping and stiffness matrices respectively. $\boldsymbol{X}$ is the vector of displacement with $\dot{\boldsymbol{X}}$ and $\ddot{\boldsymbol{X}}$ the associated velocity and acceleration vectors, $\boldsymbol{F}_{\mathrm{NL}}$ is a vector of nonlinear forces that are supposed to be regular (smooth functions) while u is a control input vector and $\boldsymbol{B}$ is the associated control matrix. The control variable u and the displacement vector $\boldsymbol{X}$ and the associated velocity and acceleration vectors $\dot{\boldsymbol{X}}$ and $\ddot{\boldsymbol{X}}$ are time-dependent. For sake of simplicity, the time variable is omitted in all equations.

It is usual to put System (1) into a space representation by defining the state vector $\boldsymbol{x}$. In mechanical systems, the state vector is built by considering displacements and velocities such as $\boldsymbol{x} = [X_1, \dot{X}_1, X_2, \dot{X}_2, ..., X_q, \dot{X}_q]^T$ with q is the number of degrees of freedom. In fact, state space representations are privileged in order to deal with observation and control issues more easily. Hence, a set of first order differential equations can be obtained as follows:

$$\dot{\boldsymbol{x}} = \boldsymbol{f}(\boldsymbol{x}, u) \tag{2}$$

Then $\boldsymbol{f} : R^n \rightarrow R^n$ is a smooth nonlinear vector field, involving the existence and the continuity of its successive derivatives. The first order derivatives are noted by: $(\nabla f)_{ij} = \frac{\partial f_i}{\partial x_j}$. $n = 2 \times q$ is the dimension of the state vector.
Let y be the single output of System (2) given by

$$y = h(\boldsymbol{x}) \tag{3}$$

where h is a smooth scalar function of the state vector $\boldsymbol{x}$, with the gradient denoted by the row vector ∇h such $(\nabla h)_i = \frac{\partial h}{\partial x_i}$. The function h is considered nonlinear to keep a general setting for the mathematical formulation. In fact, the function h is linear since the output signal we are interested by in the considered framework is in general given by a displacement, or a velocity or by an acceleration.

2.1. Problem statement

Without lose of generality, lets consider that the origin $(\boldsymbol{x}_{\mathrm{e}}, u_{\mathrm{e}}) = (\mathbf{0}, 0)$ is the equilibrium of System (2). The initial problem considered in [36] is to determine a state feedback control $u = \gamma(\boldsymbol{x})$ such that the closed loop system

$$\dot{\boldsymbol{x}} = \boldsymbol{f}(\boldsymbol{x}, \gamma(\boldsymbol{x})) \tag{4}$$

is asymptotically stable i.e. the eigenvalues of the closed loop system around its equilibrium are with strictly negative real part.

However, the implementing of the state feedback $u = \gamma(\boldsymbol{x})$ requires the state variables $x_i, (i = 1, ..., n)$ to be measurable, which is not common in practice. In fact, measures are often too costly and/or sensors can have non-negligible impact on the dynamical behaviour of the system. In these cases, state observers are recommended to be used instead of sensors for the estimating of the system states by using only the inputs and outputs of System (2). The obtained estimations will be used instead of the real variables to define the obsever based feedback control as $u = \gamma(\hat{\boldsymbol{x}})$. The problem is then to determine an estimated state vector $\hat{\boldsymbol{x}}$ to be used instead of the state vector $\boldsymbol{x}$ such that the equilibrium of the resulting closed loop system

$$\dot{\boldsymbol{x}} = \boldsymbol{f}(\boldsymbol{x}, \gamma(\hat{\boldsymbol{x}})) \tag{5}$$

is asymptotically stable.

The existence of a state observer for System (2) is conditioned by its observability [45]. The latter must be analyzed as a preliminary step before the designing of the observer. A rank condition for the observability is given in the following [44, 45].

2.2. Observability analysis

Let r_i be the relative degree of the output y with respect to the i^{th} state variable x_i, which denotes the number of necessary time derivatives of the output y to make the state variable x_i appear:

$$\begin{cases} L_{\boldsymbol{f}}^{k} h(\boldsymbol{x}) = 0 \quad \forall k < r_i - 1 \\ L_{\boldsymbol{f}}^{r_i - 1} h(\boldsymbol{x}) \neq 0 \end{cases} \tag{6}$$

where $L_{\boldsymbol{f}}^{k}h(\boldsymbol{x})$ is the k-th Lie derivative of the output $y = h(\boldsymbol{x})$ with respect to $\boldsymbol{f}$, given by $L_{\boldsymbol{f}}h = \nabla h\boldsymbol{f}$. Hence, the r_i-th time derivative of the output y can be expressed as a function in the state variables and the time-derivatives of the input u as follows:

$$y^{(r_i)} = \beta_i^{(r_i)}\left(x_{\bar{i}}, x_i, u, \dot{u}, ..., u^{(r_i-1)}\right) \tag{7}$$

with $\bar{i} = \{1, 2, ..., n\} - \{i\}$.

The vector of the output derivatives can be be expressed more generally by

$$\boldsymbol{Y}^{(\boldsymbol{r})} = \boldsymbol{\beta}^{(\boldsymbol{r})}(\boldsymbol{x}, \boldsymbol{v}) \tag{8}$$

where $\boldsymbol{\beta}^{(\boldsymbol{r})}(\boldsymbol{x}, \boldsymbol{v}) = \left[\begin{array}{ccc} \beta_1^{(r_1)}\left(x_{\bar{1}}, x_1, u, \dot{u}, ..., u^{(r_1-1)}\right) & \cdots & \beta_n^{(r_n)}\left(x_{\bar{n}}, x_n, u, \dot{u}, ..., u^{(r_n-1)}\right) \end{array}\right]$ with $\boldsymbol{v} = \left[\begin{array}{cccc} u & \dot{u} & \cdots & u^{(r_k-1)} \end{array}\right]$, $r_k = \max(r_i)$ and $\boldsymbol{Y}^{(\boldsymbol{r})} = \left[\begin{array}{ccc} y^{(r_1)} & \cdots & y^{(r_n)} \end{array}\right]$.

Hence System (2) is said observable if the Jacobian matrix associated to $\boldsymbol{\beta}^{(\boldsymbol{r})}(\boldsymbol{x}, \boldsymbol{v})$ is of full rank, that is:

$$\operatorname{rank}\left(\frac{\partial \boldsymbol{\beta}^{(\boldsymbol{r})}(\boldsymbol{x}, \boldsymbol{v})}{\partial \boldsymbol{x}}^{\mathrm{T}}\right) = n \qquad \forall \boldsymbol{x} \in R^n \tag{9}$$

3. Nonlinear state observer with the gradient descent method

A state observer for System (2) is a dynamical system which aims to estimate the state variables x_i by only exploiting the input and output of System (2) as expressed by the following equations:

$$\begin{cases} \dot{\hat{\boldsymbol{x}}} = \boldsymbol{f}(\hat{\boldsymbol{x}}, u) + \boldsymbol{\phi}\left(y, \hat{y}\right), \hat{\boldsymbol{x}}(0) = \hat{\boldsymbol{x}}_0 \\ \hat{y} = h(\hat{\boldsymbol{x}}) \end{cases} \tag{10}$$

The estimated states $\hat{x}_i$ are expected to asymptotically converge to the real states x_i when the function ϕ depending on the observer output $\hat{y}$ and the system output y tends to zero. The main question when dealing with nonlinear state observer is to define a suitable function ϕ. In this study, this function is defined as the gradient of the error between the system and observer outputs or between the high order derivatives of the system and observer outputs. These give rise to two different state observers namely the gradient descent nonlinear observer (GDNLO) and the modified GDNLO respectively

[44].

The GDNLO gives state estimations by correcting them in the direction minimizing the gradient of the squared error between the system output and the GDNLO output. This lets the dynamical behaviour of the GDNLO to be expressed as follows:

$$\begin{cases} \dot{\hat{\boldsymbol{x}}} = \boldsymbol{f}(\hat{\boldsymbol{x}}, u) + \boldsymbol{\alpha} \nabla_{\hat{\boldsymbol{x}}} \phi\left(y, \hat{y}\right); \hat{\boldsymbol{x}}(0) = \hat{\boldsymbol{x}}_0 \\ \hat{y} = h(\hat{\boldsymbol{x}}) \end{cases} \tag{11}$$

where $\nabla_{\hat{\boldsymbol{x}}} \phi\left(y, \hat{y}\right)$ is the gradient of the function ϕ:

$$\nabla_{\hat{\boldsymbol{x}}} \phi\left(y, \hat{y}\right) = -\frac{\partial h(\hat{\boldsymbol{x}})^{\mathrm{T}}}{\partial \hat{\boldsymbol{x}}} \left(y - \hat{y}\right) \tag{12}$$

with the function ϕ is defined as the quadratic error between the system and observer outputs:

$$\phi\left(y, \hat{y}\right) = \frac{1}{2} \left(y - \hat{y}\right)^2 \tag{13}$$

while $\boldsymbol{\alpha} = \mathrm{diag}\left(\alpha_1, ..., \alpha_n\right)$ is a diagonal matrix of positive integers defining the step of the gradient descent. This parameter which represents also the gain of the observer is fixed to an arbitrary diagonal matrix $[\alpha_{ii}]$ (can be chosen not diagonal) but with ensuring the stability of the dynamics of the estimation error $\tilde{\boldsymbol{x}} = \hat{\boldsymbol{x}} - \boldsymbol{x}$, defined in [44] as follows:

$$\dot{\tilde{\boldsymbol{x}}} = \left(\boldsymbol{f}_{\hat{\boldsymbol{x}}}\left(\boldsymbol{x}, u\right) - \boldsymbol{\alpha} h_{\hat{\boldsymbol{x}}}\left(\boldsymbol{x}\right)^{\mathrm{T}} h_{\hat{\boldsymbol{x}}}\left(\boldsymbol{x}\right)\right) \tilde{\boldsymbol{x}} \tag{14}$$

where $\boldsymbol{f}_{\hat{\boldsymbol{x}}} = \frac{\partial \boldsymbol{f}}{\partial \hat{\boldsymbol{x}}}$ and $h_{\hat{\boldsymbol{x}}} = \frac{\partial h}{\partial \hat{\boldsymbol{x}}}$. Hence, as the step of the gradient descent $\boldsymbol{\alpha}$ controls the stability of the dynamics of the estimation error, it should be fixed in a such manner as to obtain suitable convergence properties (convergence rate, steady state for the estimation error).This point is discussed in later when dealing with the estimating and controlling of FIV issued from the mode-coupling mechanism.

The accuracy of the state estimation of the variable x_i may be negatively impacted in particular when $\frac{\partial h(\hat{\boldsymbol{x}})}{\partial \hat{x}_i} = 0$. In this case, the output error (12) does not intervene in the estimation of x_i. To overcome this inconvenient, the following output error function can be used:

$$\phi\left(y, \hat{y}\right) = \frac{1}{2} \left(\boldsymbol{Y}^{(\boldsymbol{r})} - \hat{\boldsymbol{Y}}^{(\boldsymbol{r})}\right) \boldsymbol{W} \left(\boldsymbol{Y}^{(\boldsymbol{r})} - \hat{\boldsymbol{Y}}^{(\boldsymbol{r})}\right)^{\mathrm{T}} \tag{15}$$

where $\boldsymbol{W} = \mathrm{diag}\,(w_1, ..., w_n)$ and w_i are positive weighting coefficients of the output derivatives. Considering the new output error function, the so-called modified GDNLO can be defined. The dynamics of the corresponding i-th estimated state variable is governed by the following equation:

$$\begin{cases} \dot{\hat{x}}_i = f_i(\hat{\boldsymbol{x}}, u) + \alpha_i \sum_{l=1}^{n} w_l \frac{\partial \beta_l^{r_l}(\hat{\boldsymbol{x}}_l, \hat{\boldsymbol{x}}_{\bar{l}}, \boldsymbol{v(t)})}{\partial \hat{x}_i} \left(y^{(r_l)} - \hat{y}^{(r_l)} \right); \hat{\boldsymbol{x}}(0) = \hat{\boldsymbol{x}}_0 \\ \hat{y} = h(\hat{\boldsymbol{x}}) \end{cases} \tag{16}$$

Remark: The formal proof of the stability of the observer error system was developed in [44] and, thus, is not included in this study.

4. Application and results

In order to assess the efficiency of the proposed nonlinear state observers when used for the mitigating of mode-coupling based vibrations, their capacities to be effective in the estimating of the corresponding vibrations are first analyzed. Hence, the well known Hultèn system represented in Figure (1) and defined in [46] for the modelling of mode-coupling instabilities in drum brake systems is considered. Despite its simplicity and minimality (two-degrees of freedom), it was shown to be a suitable benchmark for a reliable capture of the mode-coupling phenomenology, which permitted numerous studies as in [9] for understanding the role of damping in mode-coupling, in [47, 17, 48] for uncertainty propagation and quantification and in [26, 36] for the mitigating of mode-coupling instabilities. Using minimal models such as the Hultèn one permits to overcome the numerical difficulties often involved by the considering of high dimensional models and thus it permits to focus mainly on the methodology. It was the spirit of numerous studies dealing with FIV [27, 49, 30, 35] and is the one in which the present study fits. So, the Hultèn model is considered in the following for the analysis of the performances of the gradient based state observers when used for the estimating and controlling of friction-induced vibrations issued from the mode-coupling mechanism. The Hultèn system and the associated stability and nonlinear dynamical behaviour are firstly presented. The GDNLO and the modified GDNLO are then applied and assessed by considering two principal objectives: the first one is related to the convergence and the accuracy of the generated estimations of the vibrations and the second consists in the performances of the

state observers when inserted in control loops defined by linearizing and stabilizing state feedback controls. Otherwise, the control scheme based on linearizing state feedbacks is not given in this study for making the paper shorter. Readers are invited to see [36] for more details.

[Figure 1 about here.]

4.1. Model description

As illustrated in Figure (1), the mechanical system consists in a mass assumed to be in a permanent contact with a moving band. The contacts are modelled by two stiffnesses with linear and nonlinear (cubic) parts. The friction coefficient μ at the contact is assumed to be constant as well as the velocity of the band. The relative velocity between the band and the velocities $\dot{X}_1$ and $\dot{X}_2$ is assumed positive which makes constant the direction of the friction force. According to the Coulomb's law, the tangential force F_{T} is assumed proportional to the normal force F_{N} that is: $F_{\mathrm{T}} = \mu F_{\mathrm{N}}$, see ([46, 9]) for more details. The second order differential equation governing the dynamic behaviour of the system can be expressed in the state space by considering the state vector

$$\boldsymbol{x} = \begin{bmatrix} x_1 \\ x_2 \\ x_3 \\ x_4 \end{bmatrix} = \begin{bmatrix} X_1 \\ \dot{X}_1 \\ X_2 \\ \dot{X}_2 \end{bmatrix}$$

, so that a system like (2) can be obtained as follows:

$$\dot{\boldsymbol{x}} = \boldsymbol{f}(\boldsymbol{x}, u) = \begin{bmatrix} x_2 \\ -w_1^2 x_1 - \eta_1 w_1 x_2 + \mu w_2^2 x_3 - \psi_1^{\mathrm{NL}} x_1^3 + \mu \psi_2^{\mathrm{NL}} x_3^3 \\ x_4 \\ -\mu w_1^2 x_1 - w_2^2 x_3 - \eta_2 w_2 x_4 - \mu \psi_1^{\mathrm{NL}} x_1^3 - \psi_2^{\mathrm{NL}} x_3^3 + u \end{bmatrix} \tag{17}$$

with the output function given by $y = h(\boldsymbol{x}) = x_1$. Otherwise, $w_i = \sqrt{k_i/m}$ are natural pulsations, $\eta_i = c_i/\sqrt{m k_i}$ are the relative damping and $\psi_i^{\mathrm{NL}} = k_i^{\mathrm{NL}}$, for $i = 1, 2$. For numerical simulation, all magnitudes are given in the MKSA (Meter (m), Kilograme (Kg), Second (s), Ampere) International System by: $w_1 = 2\pi \times 100$ rad/s, $w_2 = 2\pi \times 75$ rad/s $\eta_1 = \eta_2 = 0.02$, $\psi_1^{\mathrm{NL}} = w_1^2$, $\psi_2^{\mathrm{NL}} = 0$, $\mu = 0.4$ and $m = 1$ Kg.

4.2. Stability property and nonlinear dynamical behaviour

As previously explained in the introduction, the stability analysis and the prediction of the dynamical solutions of systems that are submitted to mode-coupling instabilities must be performed to determine if the mitigating or even the suppressing of the predicted vibrations is necessary. The stability being related to the equilibrium point, the latter must be determined by solving the static equation associated to System (17). In the studied case, it is easy to verify that $(\boldsymbol{x_e}, u_e) = (\mathbf{0}, 0)$ is the equilibrium point the local stability of which can be analysed by using the indirect Lyapunov method method [41]. Hence, $\boldsymbol{x}_e$ is said to be asymptotically stable if all the eigenvalues are with strictly negative real parts and unstable if at least one eigenvalue is with a positive real part. By applying this procedure for different values of the friction coefficient μ, the mode-coupling phenomenon is pointed out as shown in Figure (2). The system presents a couple of complex conjugate eigenvalues the imaginary parts (and thus the frequencies) of which become equal at the coalescence point ($\mu_{\mathrm{c}} \approx 0.289$) while the corresponding real parts separate. As one of the real part becomes positive, the system equilibrium becomes unstable. Consequently, for the values $\mu > \mu_{\mathrm{c}}$, when the system state is moved from its equilibrium then the system state moves far away its equilibrium with a divergence rate defined by the real parts of the unstable eigenvalues and converges to a stationary oscillating regime. As example, the temporal evolutions of the displacement x_1 and the corresponding velocity x_2 that are obtained by performing time integration of the nonlinear differential equations (17) with the initial state $\boldsymbol{x}_0(0) = [0.001, 0, 0, 0]$ and $\mu = 0.4$ are plotted in Figures (3-(a,b)) and (3-(c,d)) respectively. A periodic oscillating regime with a period $t_{\mathrm{p}} = 10^{-2}$ s and stationary amplitudes (0.563 m for the displacement x_1 and 310.7 m/s for the velocity x_2 is observed). The same observation can be made about the displacement x_3 and the corresponding velocity x_4 which also converge to the same periodic oscillating regime with the same period. In order to mitigate the predicted oscillations and since the latter are often not easily measurable in practice, they must be estimated. The gradient descent based observers (GDNLO and modified GDNLO) are developed and assessed in the following subsections.

[Figure 2 about here.]

[Figure 3 about here.]

4.3. Performance analysis of the GDNLO and the modified GDNLO

As previously presented, the existence of a state observer must be demonstrated before the design step. For this purpose, the observability of System (17) is first analyzed. In a second step, the GDNLO and modified GDNLO are determined and assessed from their capacities to be convergent and accurate when used for the estimating of the mode-coupling based vibrations. Finally, both observers are introduced in control loops based on linearizing feedbacks. Then, their performances are discussed.

4.3.1. Observability analysis

The existence of a state observer for System (17) is conditioned by the observability rank condition given by (9). The vector $\boldsymbol{\beta}$ of the successive derivatives of the system output associated to System (17) is obtained as follows:

$$\boldsymbol{\beta}(\boldsymbol{x},\boldsymbol{v}) = \begin{pmatrix} y \\ \dot{y} \\ y^{(2)} \\ y^{(3)} \end{pmatrix} \begin{pmatrix} x_1 \\ x_2 \\ -w_1^2 x_1 - \eta_1 w_1 x_2 + \mu w_2^2 x_3 - \psi_1^{\mathrm{NL}} x_1^3 \\ -\eta_1 w_1^3 x_1 + (\eta_1^2 w_1^2 - w_1^2) x_2 - \mu \eta_1 w_1 w_2^2 x_3 + \mu w_2^2 x_4 + \eta_1 w_1 \psi_1^{\mathrm{NL}} x_1^3 - 3\psi_1^{\mathrm{NL}} x_2 x_1^2 \end{pmatrix} \tag{18}$$

Then, it can be verified that the associated jacobian matrix is a full rank which proofs the observability of the Hultèn system. Hence, a state observer exists and can be designed.

4.3.2. State estimation by using the GDNLO

The GDNLO corresponding to System (17) can be built according to (11), (12) and (13). The stage a bit tricky concerns the determining of the step parameter $\boldsymbol{\alpha}$ of the gradient descent. As previously presented, this parameter is fixed such as the stability of the dynamics of the estimation error (14) is ensured. The step size of the gradient descent is chosen diagonal such as $\boldsymbol{\alpha} = \mathrm{diag}\left([\alpha_1, 0, 0, 0]^{\mathrm{T}}\right)$. The other parameters α_2, α_3 and α_4 are set to zero without loss of generality since the derivatives of the output with respect to x_2, x_3 and x_4 are equal to zero. The dynamical behaviour of the corresponding

GDNLO is given as follows:

$$\begin{cases} \dot{\hat{x}}_1 = \hat{x}_2 + \alpha_1(y - \hat{y}) \\ \dot{\hat{x}}_2 = -w_1^2\hat{x_1} - \eta_1 w_1 \hat{x_2} + \mu w_2^2 \hat{x_3} - \psi_1^{\mathrm{NL}} \hat{x}_1^3 \\ \dot{\hat{x}}_3 = \hat{x}_4 \\ \dot{\hat{x}}_4 = -\mu w_1^2 \hat{x}_1 - w_2^2 \hat{x}_3 - \eta_2 w_2 \hat{x}_4 - \mu \psi_1^{\mathrm{NL}} \hat{x}_1^3 + u \\ \hat{y} = \hat{x}_1 \end{cases} \tag{19}$$

The $\boldsymbol{\alpha}$ parameter controls the stability of the estimation errors and thus the convergence properties of the observer. In order to observe the effect of the step parameter $\boldsymbol{\alpha}$ of the gradient descent on the performances of the GDNLO, different values are considered for α_1. The estimation errors defined by $x_1 - \hat{x}_1$ are plotted in Figure (4-(a,b,c,d)) and Figure (5-(a,b)). It is useful to note that the GDNLO is initialized to the zero state $\hat{\boldsymbol{x}}(0) = [0, 0, 0, 0]^{\mathrm{T}}$. The latter being unknown, is expected to converge to the real state of the System (17). Results show that in the studies case, the parameter α_1 must be chosen neither too small, which makes the convergence of the GDNLO very slow (Figure (4)-(a,b) with $\alpha_1 = 0.5$) nor too high values may prevent the convergence of the GDNLO and makes it unstable (Figure (4)-(c,d) with $\alpha_1 = 10$). Hence, a suitable compromise must be determined. With $\alpha_1 = 4$, the stability and convergence properties of the GDNLO are more convenient. The corresponding transient regime show high amplitudes which decay more rapidly (small amplitudes are reached from 0.9 second) to reach smaller error levels as shown in Figure (5)-(a,b). It can be noted that in order to reach a level of error with $\alpha_1 = 0.5$ as in the case with $\alpha_1 = 4$, the GDNLO must be simulated for a too much longer time (80 seconds). The other estimation errors concerning the remaining state variables x_2, x_3 and x_4 are plotted in Figure (5)-(c,d,e,f,g,h). They show also high amplitudes in the transients but decay rapidly (smaller levels of amplitudes are reached after O.9 second) . In fact, all results show that the estimated displacements $\hat{x}_1$ and $\hat{x}_3$ and the corresponding estimated velocities $\hat{x}_2$ and $\hat{x}_4$ converge to the real displacements x_1 and x_3 and velocities x_2 and x_4 respectively, after short transient regimes however errors persist in the stationary regime (which corresponds to the oscillatory regime for the Hulten system). These errors may be attributed to the fact that the function of the output error does not explicitly intervene in the dynamics of the GDNLO since the system output is independent on the state variables $x_{(2,3,4)}$. Only the estimation of the displacement x_1

is clearly corrected according to the gradient descent of the output error function. The pertinence of the using of the GDNLO for the mitigating of the mode-coupling based oscillations will be discussed later in this study.

[Figure 4 about here.]

[Figure 5 about here.]

4.3.3. State estimation with the modified GDNLO

As mentioned previously, estimation errors persists in the stationary regime characterized by limit cycle oscillations. They may be related to the fact that the function of the output error only intervenes in the estimation of the displacement x_1. To make the output error more important in the estimation dynamics, the modified GDNLO is considered with $\boldsymbol{\alpha} = [10^{-4}, 10^{-4}, 0, 0]^{\mathrm{T}}$ and $v_3 = 10^{-2}$ and $v_4 = 0$. The corresponding dynamics is governed by the following equations:

$$\begin{cases} \dot{\hat{x}}_1 = \hat{x}_2 + \alpha_1 \left[v_3 \left(-w_1^2 - 3\psi_1^{\mathrm{NL}} \hat{x}_1^2 \right) \left(y^{(2)} - \hat{y}^{(2)} \right) \right] \\ \dot{\hat{x}}_2 = -w_1^2 \hat{x}_1 - \eta_1 w_1 \hat{x}_2 + \mu w_2^2 \hat{x}_3 - \psi_1^{\mathrm{NL}} \hat{x}_1^3 + \alpha_2 \left[-v_3 \eta_1 w_1 \left(y^{(2)} - \hat{y}^{(2)} \right) \right] \\ \dot{\hat{x}}_3 = \hat{x}_4 \\ \dot{\hat{x}}_4 = -\mu w_1^2 \hat{x}_1 - w_2^2 \hat{x}_3 - \eta_2 w_2 \hat{x}_4 - \mu \psi_1^{\mathrm{NL}} \hat{x}_1^3 + u \end{cases} \tag{20}$$

The estimation errors given by the modified GDNLO (20) are plotted in Figure (6)(a-h). Results show better convergence properties for the modified GDNLO than those observed with the GDNLO. The high estimation errors previously observed with the GDNLO transient are strongly mitigated. For example, the maximal estimation error $x_1 - \hat{x}_1$ is reduced with a high ratio (10^3). In fact, the taking into account of the error between the output derivatives of the system and the modified GDNLO, has permitted the anticipating the errors induced by the gap between the initial states of the system and the modified GDNLO. This has required a smaller step gradient. The accuracy at the stationary regime of the modified GDNLO is also better than the accuracy given by the GDNLO. Indeed, it can be observed that the corresponding estimation errors converge to values close to zero (the estimation errors are strongly reduced compared to those obtained with the GDNLO). This shows the asymptotic convergence of the modified GDNLO.

[Figure 6 about here.]

4.4. The GDNLO and modified GDNLO within nonlinear control loops for the controlling of FIV

The aimed purpose behind the using of the GDNLO or the modified GDNLO is to determine estimations of the system oscillations occasioned by mode-coupling. These estimations are going to be used instead of measures (that are, in numerous practical cases, difficult to be performed and/or too costly) in order to implement state feedbacks mitigating or suppressing the oscillations. Performances of the GDNLO and the modified GDNLO when used in control loops are analyzed in the following. For this purpose, the input-state linearizing feedback which was developed and determined in [36] is implemented by using the GDNLO and the modified GDNLO. For sake of brevity, the procedure which permits to determine the input-state linearizing feedback for System (17) is not given in this study. All details about this point are given in the previous study of the author [36]. The main idea is to determine a nonlinear coordinate transformation which algebraically puts System (17) into a linear canonical form, the control of which is reduced to a classical pole placement problem. The nonlinear coordinate transformation was obtained as follows:

$$\begin{cases} z_1 = x_1 \\ z_2 = x_2 \\ z_3 = -w_1^2 x_1 - \eta_1 w_1 x_2 + \mu w_2^2 x_3 - \psi_1^{\mathrm{NL}} x_1^3 \\ z_4 = \eta_1 w_1^3 x_1 + \left(\eta_1^2 w_1^2 - w_1^2\right) x_2 - \eta_1 w_1 w_2^2 \mu x_3 + \mu w_2^2 x_4 + \eta_1 w_1 \psi_1^{\mathrm{NL}} x_1^3 - 3\psi_1^{\mathrm{NL}} x_2 x_1^2 \end{cases} \tag{21}$$

While the stabilizing feedback was determined as

$$v_{\mathrm{stab}} = -k_0 z_1 - k_1 z_2 - k_2 z_3 - k_3 z_4 \tag{22}$$

where the constant coefficients k_i are determined so the state matrix of the closed loop system is Hurwitz. The eigenvalues are chosen to be placed at the positions given by $-20 \pm j200$, -5 and -80.

For the implementing of the determined nonlinear state feedback, the GDNLO and the modified GDNLO previously determined are considered. Hence, the corresponding estimated state variables are used instead of the original state variables.

4.4.1. Control with the GDNLO

The estimation errors $x_i - \hat{x}_i, (i = 1, ..., 4)$ given by the GDNLO in the closed loop configuration are plotted in Figure (7)-(a,b,c,d).The convergence properties of the previously determined GDNLO are drastically deteriorated. The GDNLO is clearly unsuitable for the control objective. The separation principle which consists in the independence of the calculation of the GDNLO from the calculation of the feedback control, is not verified. This has lead to unstable closed loop behaviour when the state variables are replaced by their estimations in the control loop. The performed simulation attests the non-convenience of the previous GDNLO to be used for the mitigating of the mode-coupling based oscillations.

[Figure 7 about here.]

4.4.2. Control with the modified GDNLO

The performance of the modified version used in the closed loop configuration is evaluated. The estimation errors on the displacements and velocities are plotted in Figure (8)(a,b,c,d). By opposite to the GDNLO, results show asymptotic convergence for the modified GDNLO in the closed loop. All the estimation errors converge to zero after short transients. The convergence of the modified GDNLO is not significantly impacted when introduced in the control loop. As shown in Figure (9), the performance of the nonlinear state feedback based on the original state variables is lightly modified when the control law is determined by using the estimated state variables. The controlled displacement x_1 obtained by using the modified GDNLO is made asymptotically stable but with a lightly longer transient than the same controlled displacement obtained by using the system variables. The including of the high order derivatives of the output errors in the dynamics of the modified GDNLO has drastically enhanced the performances of the previous GDNLO in closed loop configuration. The separation principle is verified with the modified GDNLO. It has permitted the suppression of the mode-coupling based vibrations.

[Figure 8 about here.]

[Figure 9 about here.]

4.5. Robustness of the modified GDNLO based controller

In order to analyse the robustness of the proposed modified GDNLO based controller of FIV, the closed loop system is simulated by considering a noisy measured output. The measured output is assumed to be tainted by a Gaussian noise of zero mean and different variances as plotted in Figure (10-a) where few periods of oscillations are represented. The controlled displacement x_1 corresponding to the noisy output is plotted in Figure (10-b).

Results in Figure (10-b) show a non-negligible sensitivity of the control performance with respect to the noise level in the output. Indeed, the closed loop system becomes more unstable with the increase of the variance of the Gaussian noise. The asymptotic stability is lost. The original vibrations that were suppressed Figure (9) reappear when the system output is submitted to noise. These vibrations are mitigated with a ratio becoming increasingly bad by augmenting the level of the measurement noise. The asymptotic stability of the closed loop system is not robust with respect to the considered disturbances. However, the attenuation level of the vibration amplitudes also depends on the level of measurement noise.

[Figure 10 about here.]

5. Conclusion

This study has presented a nonlinear approach for the estimating and controlling of friction-induced vibration (FIV) in particular those generated from the mode-coupling mechanism. The main perspective is to analyse the efficiency of gradient descent nonlinear observers when used for the mitigating of mode-coupling based instabilities. The GDNLO considering only the gradient of the squared error between the system and observer outputs is shown to be unsuitable when used in the closed loop despite its acceptable accuracy in the estimating of the mode-coupling based vibrations. Hence, the modified GDNLO which considers the gradient of the squared errors between high order derivatives of the system and observer outputs has shown better and suitable convergence properties in both the estimating of the mode-coupling based vibrations and also when inserted in the closed loop and the vibrations were efficiently suppressed.

Otherwise, other nonlinear state observers may be considered. Indeed, the literature refers to numerous methods for nonlinear state estimation. So, it would be useful to analyze and investigate, through a comparative study, performances of other existing nonlinear state observers and to determine which one can be more effective when dealing with the controlling of friction-induced vibrations.

This study has focused on the estimating and controlling of mode-coupling based vibrations by using a minimal model. The main perspective is then to generalize this approach to real world systems. Numerical difficulties would be occasioned in particular by high dimension aspects. Associating the proposed approach together with reduced order models should be the way to privilege in order to ensure the efficiency of the proposed observer based controller of mode-coupling instabilities. Otherwise, the proposed approach has shown a non-negligible sensitivity to noisy output measurement. It is then necessary to be improved for satisfying higher robustness levels.

6. References

[1] R.A. Ibrahim. Friction-induced vibration, chatter, squeal, and chaos part 1: mechanics of contact and friction. *Am Soc Mech Eng Appl Mech Rev*, 47(7):209–226, 1994.

[2] R.A. Ibrahim. Friction-induced vibration, chatter, squeal, and chaos part 2: dynamics and modeling. *Am Soc Mech Eng Appl Mech Rev*, 47(7):227–263, 1994.

[3] G. Sheng. *Friction-induced vibration and sound: priciples and applications*. CRC Press, Boca Raton, 2008.

[4] B. Armstrong-Helouvry, P. Dupont, and C. Canudas de Wit. A survey of models, analysis tools, and compensation methods for the control of machines with friction. *Automatica*, 30:1083–1138, 1994.

[5] Hinrichs, N, Oestreich, M, and Popp, K. On the modeling of friction oscillators. *Journal of Sound and Vibration*, 216:435–459, 1998.

[6] J.J. Thomsen. Using fast vibrations to quench friction-induced oscillations. *Journal of Sound and Vibration*, 228:1079–1102, 1999.

[7] Y. Li and Z.C. Feng. Bifurcation and chaos in friction-induced vibration. *Communication Nonlinear Science Numerical Simulation*, 9:633–647, 2004.

[8] N. M. Kindkaid, O. M. O'Reilly, and P. Papadopoulos. Automative disc brake squeal. *Journal of Sound and Vibration*, 267:105–166, 2003.

[9] J-J. Sinou and L. Jézéquel. Mode coupling instability in friction-induced vibrations and its dependency on system parameters including damping. *European Journal of Mechanical A/Solid*, 26:107–122, 2007.

[10] A.R. AbuBakar and H. Ouyang. Complex eigenvalue analysis and dynamic transient analysis in predicting disc brake squeal. *International Journal of Vehicle Noise and Vibration*, 2:143–155, 2006.

[11] N. Hoffmann and L. Gaul. Effects of damping on mode-coupling instability in friction induced oscillations. *ZAMM - Journal of Applied Mathematics and Mechanics*, 83(8):524–534, 2003.

[12] H. Hetzler, D. Schwarzer, and W. Seemann. Analytical investigation of steady-state stability and hopf-bifurcations occuring in sliding friction oscillators with application to low-frequency disc brake noise. *Communication Nonlinear Science Numerical simulation*, 12:83–99, 2007.

[13] N. Coudeyras, S. Nacivet, and J-J. Sinou. Periodic and quasi-periodic solutions for multi-instabilities involved in brake squeal. *Journal of Sound and Vibration*, 328:520–540, 2009.

[14] V. Pilipchuk, P. Olejnik, and J. Awrejcewicz. Transient friction-induced vibration in a 2-dof model of brakes. *Journal of Sound and Vibration*, 334:297–312, 2015.

[15] T. Bultin and J. Woodhouse. Friction-induced vibration: quantifying sensitivity and uncertainty. *Journal of Sound and Vibration*, 329(1-2):509–526, 2010.

[16] S. Oberst and J.C.S. Lai. Statistical analysis of brake squeal noise. *Journal of Sound and Vibration*, 330(12):2978–2994, 2011.

[17] L. Nechak, S. Berger, and E. Aubry. Wiener haar expansion for the modeling and prediction of the dynamic behavior of self-excited nonlinear uncertain systems. *ASME Journal of Dynamic Systems, Measurement, and Control*, 134(5):051011, 2012.

[18] A. Nobari, H. Ouyang, and P. Bannister. Statistics of complex eigenvalues in friction-induced vibration. *Journal of Sound and Vibration*, 338:169–183, 2015.

[19] E. Denimal, L. Nechak, J-J. Sinou, and S. Nacivet. Kriging surrogate models for predicting the complex eigenvalues of mechanical systems subjected to friction-induced vibration. *Shock and Vibration*, 2016:ID 3586230, 22 pages, 2016.

[20] A. Nobari, H. Ouyang, and P. Bannister. Uncertainty quantification of squeal instability via surrogate modelling. *Mechanical Systems and Signal Processing*, 60-61:887–908, 2015.

[21] L. Nechak and J-J. Sinou. Hybrid surrogate model for the prediction of uncertain friction-induced instabilities. *Journal of Sound and Vibration*, 126:122–143, 2017.

[22] E. Denimal, L. Nechak, J-J. Sinou, and S. Nacivet. A novel hybrid surrogate model and its application on a mechanical system subjected to friction-induced vibration. *Journal of Sound and Vibration*, 434:456–474, 2018.

[23] F. Massa, H. Quan Do, T. Tison, and O. Cazier. Uncertain friction-induced vibration study:coupling of fuzzy logic, fuzzy sets and interval theories. *ASME Journal of Risk Uncertainty*, Part B:12 pages, 2015.

[24] S. Chatterjee. Non-linear control of friction-induced self-excited vibration. *International Journal of Nonlinear Mechanics*, 42:459–469, 2007.

[25] K. Popp and M. Rudolph. Vibration control to avoid stick-slip motion. *Journal of Vibration and Control*, 10:1585–1600, 2004.

[26] B. Bergeot, S. Berger, and S. Bellizzi. Mode coupling instability mitigation in friction systems

by means of nonlinear energy sinks: numerical ighlighting and local stability analysis. *Journal of Vibration and Control*, 24(15):3487–3511, 2017.

[27] H. Ouyang. Prediction and assignment of latent roots of damped asymmetric systems by structural modifications. *Mechanical Systems and Signal Processing*, 23(6):1920–1930, 2009.

[28] B. Armstrong-Helouvry and B. Amin. Pid control in the presence of static friction:a comparison of algebraic and describing function analysis. *Automatica*, 32:679–692, 1996.

[29] R.H.A. Hensen, M.J.G. Van De Molengraft, and M. Steinbuch. Friction-induced hunting limit cycles: an event mapping approach. In *Proceeding of the 2002 American Control Conference, Anchorage, AK*, pages 2267–2272, 2002.

[30] K. V. Singh and H. Ouyang. Pole assignment using state feedback with time delay in friction-induced vibration problems. *Acta Mechanica*, 224(3):645–656, 2012.

[31] A. Saha, B. Bhattacharya, and P. Wahi. A comparitive study on the control of friction-driven oscillations by time- delayed feedback. *Nonlinear Dynamics*, 60:15–37, 2010.

[32] J. Das and A. K. Mallik. Control of friction driven oscillation by time-delayed state feedback. *Journal of Sound and Vibration*, 297(3-5):578–594, 2006.

[33] S. Chatterjee. Time-delayed feedback control of friction-induced instability. *International Journal of Nonlinear Mechanics*, 42:1143–1127, 2007.

[34] M. G. Tehrani and H. Ouyang. Receptance-based partial pole assignment for asymmetric systems using state-feedback. *Shock and Vibration*, 19(5):1135–1142, 2012.

[35] Y. Liang, H. Yamaura, and H. Ouyang. Active assignment of eigenvalues and eigen-sensitivities for robust stabilization of friction-induced vibration. *Mechanical Systems and Signal Processing*, 90:254–267, 2017.

[36] L. Nechak. Nonlinear control of friction-induced limit cycle oscillations via feedback linearization. *Mechanical Systems and Signal Processing*, 126:264–280, 2019.

[37] B. Friedland and S. Mentzelopoulou. On adaptive friction compensation without velocity measurement. In *Proceeding of the First IEEE Conference on Control Applications,Dayton, OH, USA*, pages 1076–1081, 1992.

[38] N. Mallon, N. Van de Wouw, D. Putra, and H. Nijmeijer. Friction compensation in a controlled one-link robot using reduced order observer. *IEEE Transaction On Control Systems Technology*, 14:374–383, 2006.

[39] G. Ferretti, G. Magnani, and P. Rocco. Alternatives in precise load motion control of two-mass servomechanisms. In *Proceeding of the 2001 IEEE/ASME Conference on Advanced Intelligent Mechatronics, Como, Italy*, page 893898, 2001.

[40] H.I. Basturk. Observer-based boundary control design for suppression of stick-slip oscillations in drilling systems with only surface measurements. *Journal of Dynamic Systems Measurement and Control*, 139:1–7, 2017.

[41] H. Khalil. *Nonlinear Systems*. Prentice Hall, 2002.

[42] M. Arcak and P. Kokotovic. Nonlinear observers: a circle criterion design and robustness analysis. *Automatica*, 37:1923–1930, 2001.

[43] A. Atassi and H. K. Khalil. A separation principle for the stabilization of a class of nonlinear systems. *IEEE Transaction on Automatic Control*, 44:1672–1687, 1999.

[44] K. Shimizu. Nonlinear state observers by gradient descent method. In *Proceeding of the 2000 IEEE International Conference on Control Applications, Alaska, USA*, pages 616–622, 2000.

[45] A. Isidori. *Nonlinear Control Systems*. Springer-Verlag, 1993.

[46] J. Hult èn. Drum brake squeal- a self exciting mechanism with constant friction. In *In the SAE truck and bus meeting, 1993, Detroit, MI, USA SAE paper*, page 932965, 1993.

[47] L. Nechak, S. Berger, and E. Aubry. Wiener askey and wiener haar expansions for the analysis and prediction of limit cycle oscillations in uncertain nonlinear dynamic friction systems. *ASME Journal of Computational and Nonlinear Dynamics*, 9(2):021007, 2014.

[48] E. Sarrouy, O. Dessombz, and J.-J. Sinou. Stochastic study of non-linear self-excited system with friction. *European Journal of Mechanics A/Solids*, 40(2):1–10, 2013.

[49] H. Ouyang. Pole assignment of vriction-induced vibration for stabilisation through state-feedback control. *Journal of Sound and Vibration*, 329(11):1985–1991, 2009.

List of Figures

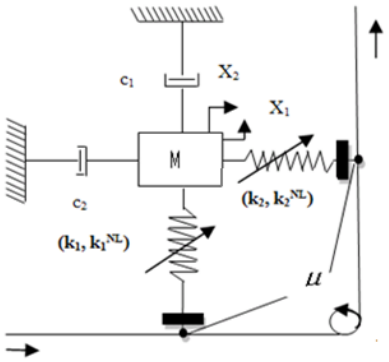

Figure 1: Mechanical system

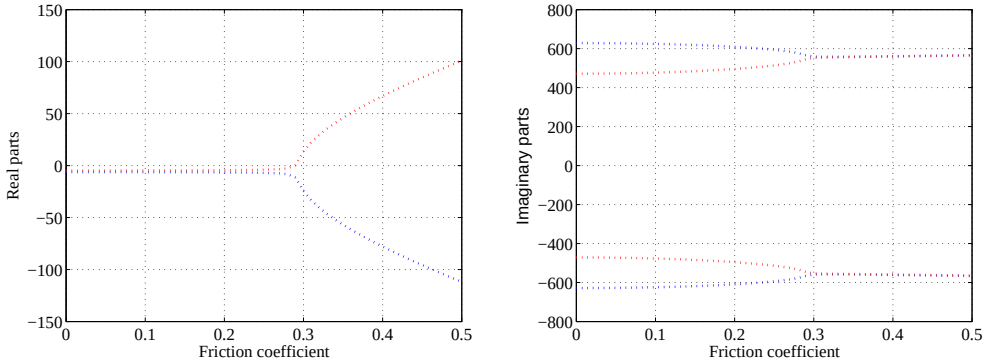

(a) (b)

Figure 2: Evolution of the eigenvalues of the Hultèn system linearized around the origin $\boldsymbol{x}_e = (\mathbf{0}, 0)$, versus the friction coefficient μ

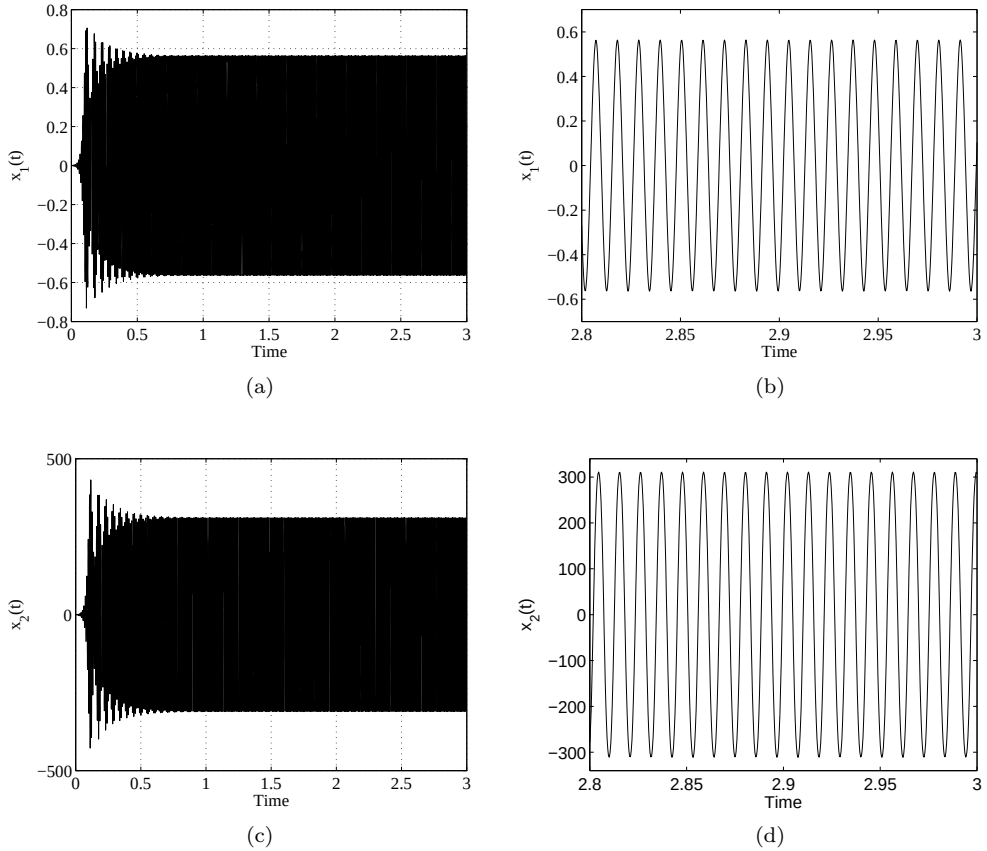

Figure 3: Temporal evolutions of: (a) the displacement $x_1(t)$ and (b) the velocity $x_2(t)$ versus time. (b) and (d) represent zooms on few periods of oscillations of $x_1(t)$ and $x_2(t)$ respectively

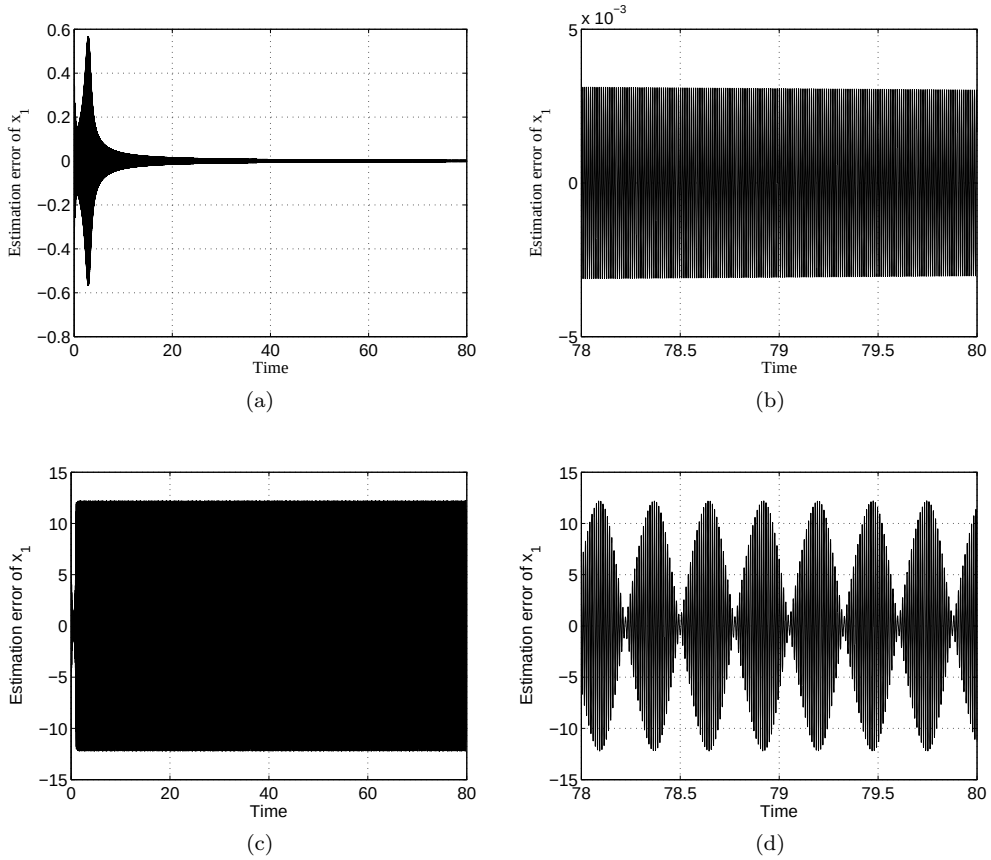

Figure 4: The estimation error $x_1 - \hat{x}_1$ of the GDNLO with $\alpha_1 = 0.5$-(a,b) and $\alpha_1 = 10$ -(c,d)

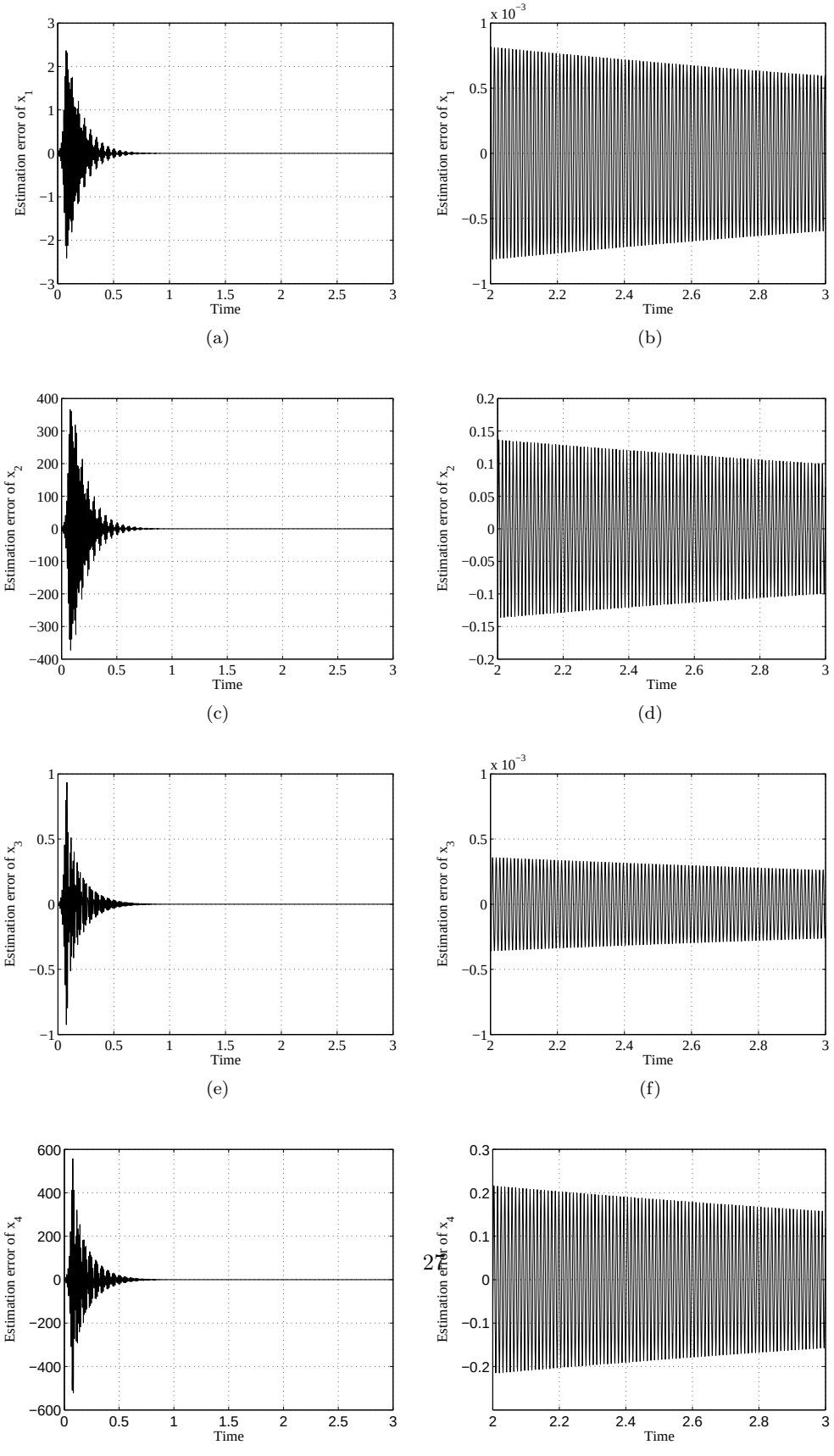

Figure 5: Estimation errors $x_i - \hat{x}_i, (i = 1, ..., 4)$ of the GDNLO with $\alpha_1 = 4$

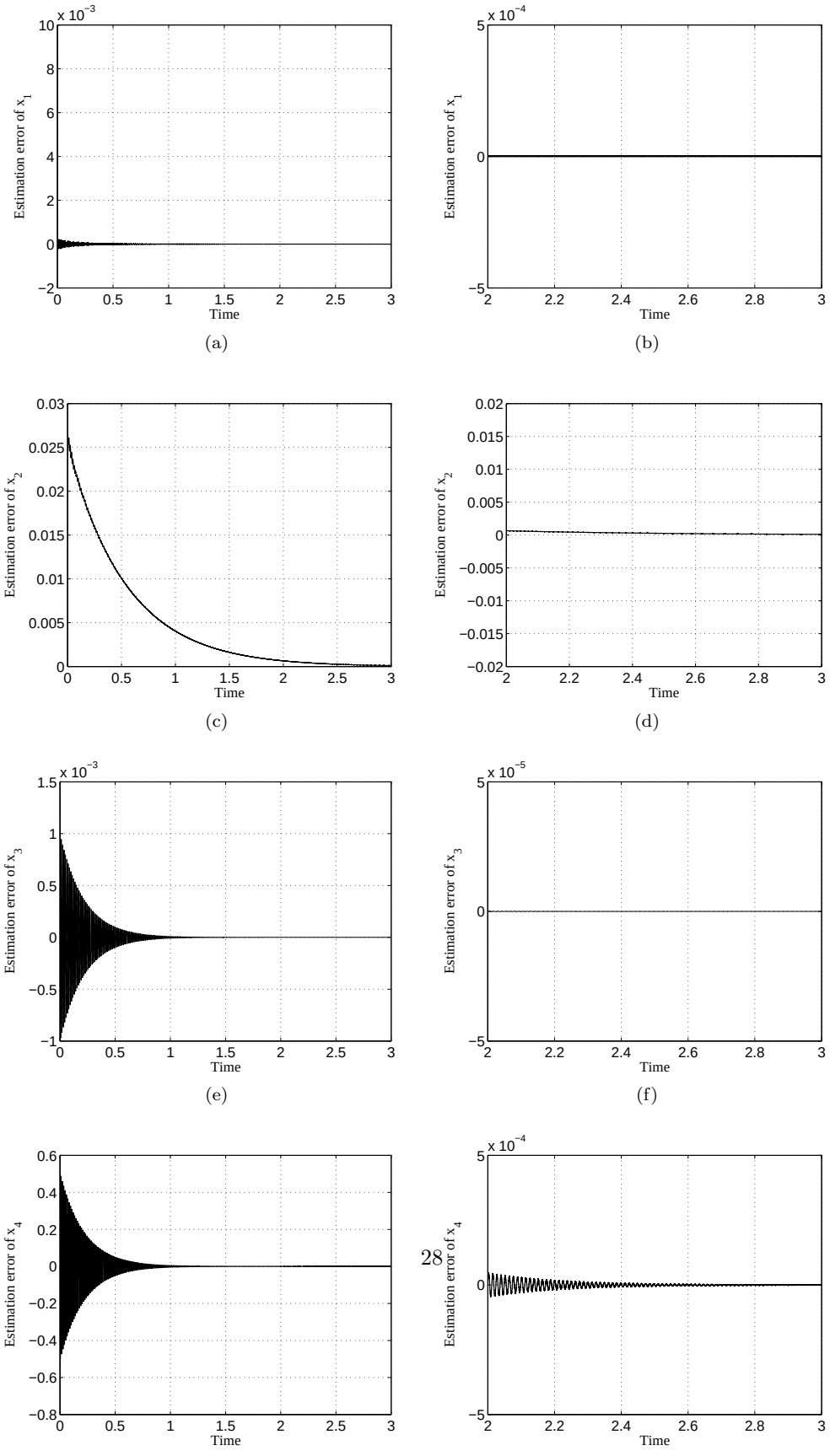

Figure 6: Estimation errors $x_i - \hat{x}_i, (i = 1, ..., 4)$ of the modified GDNLO

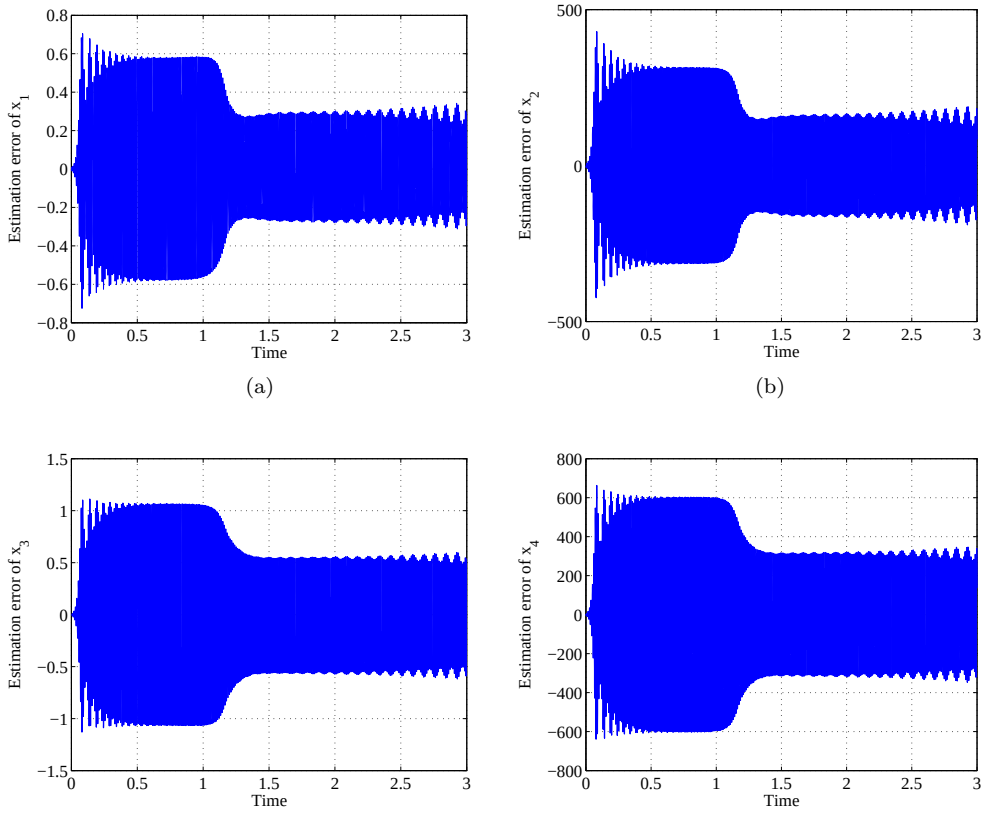

Figure 7: The estimation errors $x_i - \hat{x}_i$ of the GDNLO in the closed loop configuration

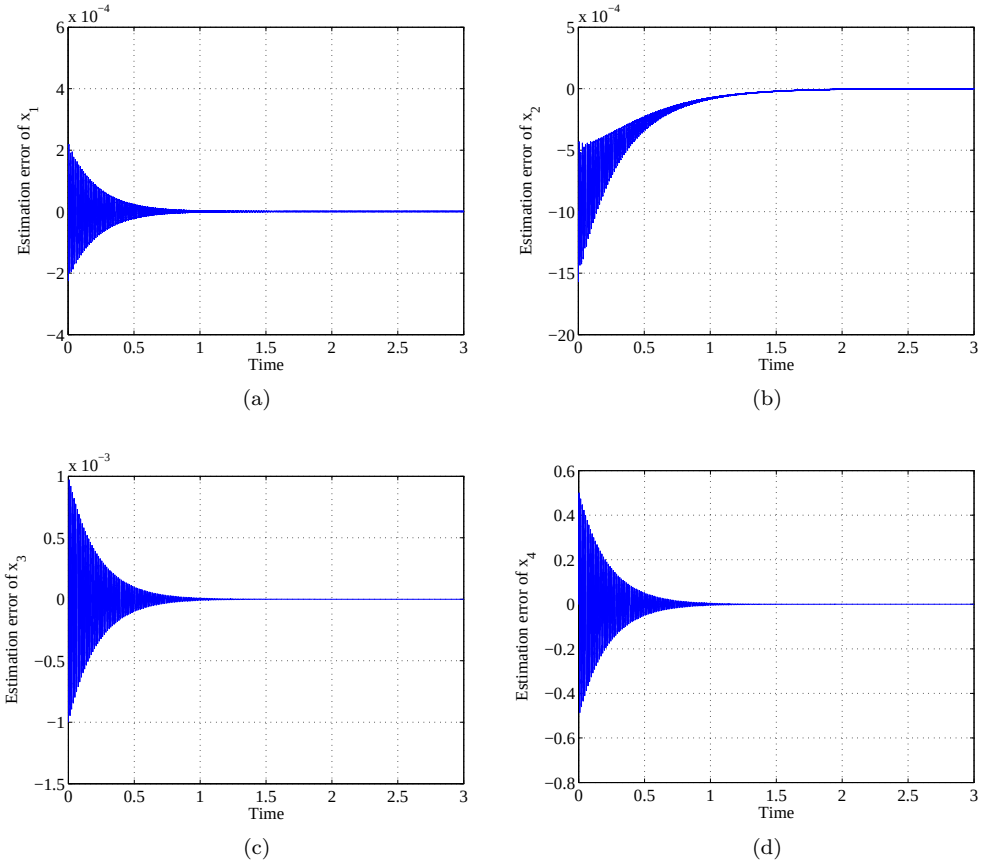

Figure 8: The estimation errors $x_i - \hat{x}_i$ of the modified GDNLO in the closed loop configuration

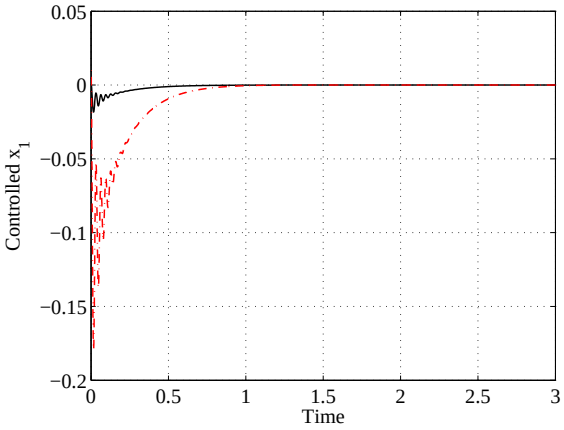

Figure 9: The controlled displacement x_1; solid line: without the modified GDNLO, dashed line: with the modified GDNLO

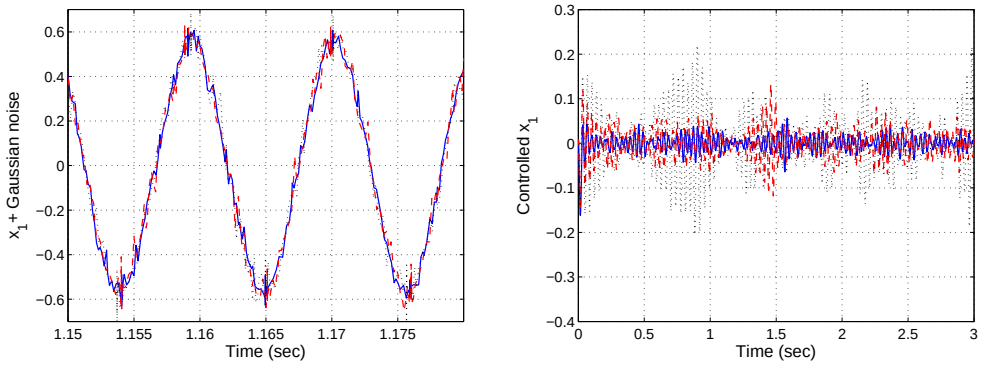

(a) (b)

Figure 10: (a)-The uncontrolled noisy displacement x_1 ; (b)- the controlled displacement x_1 ; solid line: variance = 0.001, dashed line: variance=0.002, dot line: variance=0.003